International Conference on Applied Energy 2019
Aug 12-15, 2019, Västerås, Sweden
Paper ID: 1047

CONCEPTUAL THERMO-FLUID DYNAMIC DESIGN OF THE COOLED SUPERCRITICAL CO_2 TURBINE FOR THE ALLAM CYCLE

R. Scaccabarozzi[1,2*], E. Martelli[1], M. Gatti[1,2], P. Chiesa[1], M. Pini[3], C. M. De Servi[4]

1 Politecnico di Milano, Department of Energy, via Lambruschini 4, 20156 Milan, Italy
2 Laboratorio Energia & Ambiente Piacenza (LEAP), via Nino Bixio 27/C, 29121 Piacenza, Italy
3 Delft University of Technology, Aerospace Engineering Faculty, Propulsion & Power, Kluyverweg 1, 2629 HS Delft, The Netherlands
4 Flemish Institute for Technological Research (VITO), Boeretang 200, 2400 Mol, Belgium

ABSTRACT
This paper documents the conceptual design and performance assessment of the cooled turbine of the Allam cycle. A conceptual fluid-dynamic design model is combined with a blade cooling model capable of dealing with unconventional fluids and implementing several cooling technologies. Preliminary results for a 600 MW turbine with 6 stages indicate that 5 stages need to be cooled and the film cooling effectiveness is severely limited by the high Reynolds number of the main stream.

Keywords: Allam cycle, supercritical CO_2 turbine, blade-cooling model, 1D thermo-fluid dynamic design, expander performance analysis.

NOMENCLATURE

Symbols	
a_t	Ratio between total gas heat transfer area (including the shrouds) and the blade surface
D_0	Equivalent diameter of the blade leading edge
E_f	Enhancement factor of the coolant convective heat transfer coefficient
h	Convective heat transfer coefficient
h_t	Total enthalpy
h/D_m	Ratio between the blade height and the mean diameter
I_f	Cooling channel interference factor
r_{fc}	Ratio between the film cooling and total coolant mass flow rates
t	Thickness
W	Molar weight
x/c	Ratio between the distance from the injection location and the chord length
α	Coolant injection angle
η	Overall cooling effectiveness
η_{ad}	Efficiency referred to the adiabatic availability of the system
η_{fc}	Film cooling effectiveness
λ	Ratio between the gas heat transfer and cross-sectional areas
ξ	Ratio between the coolant and gas mass flow rates
σ	Solidity
Ψ_g	Parameter accounting for the reduction of the gas cross-sectional area due to the blade thickness
Subscripts	
am	After the mixing process
aw	Adiabatic wall
bw	Blade metal wall
$bmax$	Blade metal wall maximum value
c	Coolant
g	Gas
gf	Gas at film cooling temperature
i	Inlet
o	Outlet
TBC	Thermal barrier coating
tt	Total-total
ts	Total-static
x	Direction along the flat surface
∞	Approaching
θ	Cylinder tangential direction

1. INTRODUCTION

Among the Carbon Capture and Storage (CCS) technologies, oxy-combustion cycles appear to be promising for future power generation due to their theoretical zero emissions of both pollutants and carbon

Selection and peer-review under responsibility of the scientific committee of the 11th Int. Conf. on Applied Energy (ICAE2019).

dioxide as a consequence of their closed/semi-closed configuration [1].

The comparison between the main natural-gas-fired oxy-combustion cycles reported in [2] showed that the Allam cycle [3] achieves the highest electrical efficiency (55.1 $\%_{LHV}$) and the lowest specific investment cost (1320 €/kW_{el}). Also the part-load performance appears to be quite promising according to [4]. The analysis focused on the off-design operation shows that the penalty in terms of performance reduction at partial load is less severe compared to a state-of-the-art combined cycle without CO_2 capture (in terms of the ratio between the part-load and full-load net electric efficiency).

The Allam cycle is a semi-closed, intercooled, and highly regenerative oxy-combustion cycle, which uses a CO_2 rich stream as working fluid. According to the cycle optimization performed in [5] and latest data available for the demonstration plant [6], the combustor oxidizes the fuel at about 30 MPa, producing a hot stream at about 1373 - 1473 K, which is expanded down to 3 MPa, in a cooled turbine.

The most critical cycle components are those operating at high temperatures:

- The regenerator which transfers a very large thermal duty (between 100 % and 200 % of the net power output of the cycle) with a small temperature difference between hot flue gases exiting the turbine and the mixture of oxidizer and moderator, a high pressure difference, and water condensation in flue gases (causing corrosion issues) [5].
- The combustor, which has to be operated with a diffusive flame, instead of a premixed one, to achieve a stable operation [7].
- The cooled turbine which treats a high density fluid (more than 15 times denser than a conventional gas turbine) with real gas effect [6].

The thermodynamic analysis and optimization of the cycle reported in [5] has shown that the turbine performance (in terms of efficiency and cooling flow requirement) has a considerable effect on the overall cycle efficiency. For instance, the average increase of one percentage point of the turbine stage isentropic efficiency causes a gain in the net plant efficiency of 0.325 percentage points. Similar effect is caused by the cooling systems effectiveness, each percentage point gain produces an increase of the net cycle efficiency of 0.025 percentage points. Hence, it is of crucial importance to have a reasonable estimate of the turbine design, cooling flow requirements and fluid-dynamic efficiency. To this purpose, this study proposes a methodology for the preliminary aero-thermal design of the turbine and assessment of its efficiency and cooling flow requirement.

2. OBJECTIVES OF THE STUDY

The aero-thermal design of a cooled turbine (e.g., gas turbines ones) is a challenging multidisciplinary design problem. It has to take into account not only the minimization of fluid-dynamic losses but also the design of the cooling system [8] under the condition that the mechanical integrity of either the fixed and rotating parts is guaranteed (vane and rotor blades). For this reason, the design process of these machines usually involves the concurrent use of calibrated multi-disciplinary models of increasing degree of fidelity, i.e., from conceptual to 3D CFD/FEM, possibly supplemented by extensive experimental campaigns. When assessing the performance of novel cycles (like the Allam cycle), it is necessary to perform a preliminary evaluation of the turbine efficiency and cooling flow requirement relying on a few (or even without) experimental data. This need has motivated the development of simplified models capable of estimating the cooling flow requirements and induced losses for conventional gas turbines [9–11]. These models rely on the assumption of ideal gases behavior of the working fluid and assume typical geometrical characteristics (e.g., blade aspect ratio, solidity etc.) and flow-related parameters (velocity, heat transfer coefficients, etc.) of conventional gas turbines (using air as working fluid). Hence, such models are arguably not directly applicable to the turbine of the Allam cycle as it is necessary to take into account the effects of the extremely dense working fluid on the heat transfer coefficients (due to the higher Reynolds numbers) and turbine geometry (lower blade heights, different optimal fluid-dynamic design, etc.).

In this article, we propose a simplified methodology to preliminary assess:

- The design of the turbine (number of stages, stage loads, 1D velocity triangles, etc.).
- The turbine fluid-dynamic performance.
- The cooling flow requirements.
- The impact of the cooling system on the overall turbine performance.

The analysis of the mechanical integrity of the blade will be object of a future work.

3. METHODOLOGY

The fluid dynamic design has been performed with

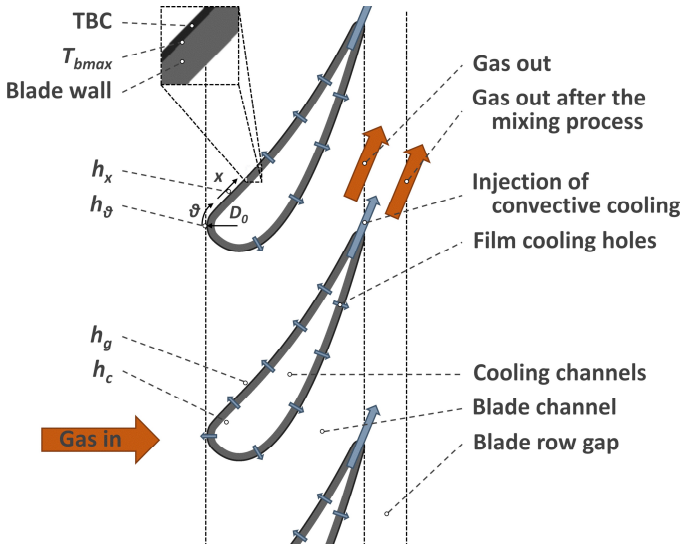

Figure 1: Representation of the cooling system model including blade channels and the mixing process occurring downstream of the blades.

zTurbo, an in-house Fortran code developed by Pini et al. [12] for the preliminary fluid-dynamic design of turbines operating with non-conventional fluids [13]. To properly evaluate the thermo-physical properties of the working fluid, zTurbo has been linked to FluidProp [14], a library which implements models for pure fluids and mixtures, featuring reasonable accuracy for the mixtures and operating ranges of interest (i.e., CO_2-rich). Even though no experimental campaign was performed to calibrate the equation of state on the specific composition used in this work, FluidProp implements state-of-the-art correlation for this type of working fluid, such as the GERG-2008 equation of state [15].

In this work, the Traupel loss correlation [16] was used to estimate the fluid-dynamic losses, while the blade number was computed using the Zweifel loading criterion [17].

As for the prediction of the cooling flow requirement and its effect on the turbine efficiency, a cooling system model has been developed and integrated in the zTurbo code. The model is an extension of the one originally proposed by [9], and allows one to design a turbine stage considering the concurrent presence of convective cooling, film cooling, and thermal barrier coating (TBC), or any combination of these (as specified by the user). The model described in the following is represented in Figure 1, and is valid for each stator and rotor of each cooled stage. The model allows the user to set the main geometrical and material-related parameters (e.g., $D_{H,c}$, t_{bw}, k_{bw}, t_{TBC}, k_{TBC}, etc.) used in the computational process, assuming:

- The maximum allowable metal temperature (T_{bmax}), set by the user, is constant in each point of the external metal blade surface.
- The coolant injection does not change the direction of the gas velocity at the exit of the blade row with respect to the uncooled computation.

First, for each blade cascade, the need for blade cooling is verified checking if the recovery temperature of the mainstream is higher than the allowed maximum temperature of the metal. If it is higher, the iterative procedure starts by assuming a first guess value for the overall cooling effectiveness (η) and computing the coolant outlet temperature ($T_{c,o}$) (from the definition of effectiveness Eq. (1)) and the coolant inlet temperature ($T_{c,i}$), to be defined by the user depending on the available cold streams of the cycle:

$$\eta = \frac{T_{c,o} - T_{c,i}}{T_{bmax} - T_{c,i}} \tag{1}$$

Then, the correlation by Dittus and Boelter [18] (Eq. (2)) and the average coolant properties between the inlet ($T_{c,i}$) and outlet ($T_{c,o}$) temperature are used to compute the convective heat transfer coefficient (h_c) inside the cooling channels (Eq. (3)), where the heat transfer process is enhanced by a factor (E_f) related to the internal geometry of the cooling channels.

$$Nu_c = E_f Re_c^{0.8} Pr_c^{0.4} \tag{2}$$

$$h_c = Nu_c \frac{k_c}{D_{H,c}} \tag{3}$$

h_c is then used to update the value of the overall cooling effectiveness in the iterative process, according to Eq. (4) considering a geometrical interference factor (I_f), accounting for the reduction of the available heat transfer area of the cooling channels [9].

$$\eta = 1 - e\wedge\left\{\frac{\left(\frac{1}{h_c} + \frac{t_{bw}}{k_{bw}}\right)^{-1} I_f A_c}{\frac{\dot{m}_c \Delta h_{t,c}}{T_{c,o} - T_{c,i}}}\right\} \tag{4}$$

The row is virtually divided between the film cooling zone (i.e., the blade channel) and the mixing zone (i.e., the gap between the rows). In the film cooling zone, Eqs. (5) and (6) are applied to compute respectively the gas outlet total enthalpy and the velocity ($v_{g,am}$) after the mixing process with the film cooling mass flow rate. In the mixing zone, the same equation are used to compute

the properties at the blade row exit where the gas stream is mixed also with the remaining convective cooling mass flow rate, as shown in Figure 1. The momentum balance equation (Eq. (6)) considers as outlet conditions (before the mixing process in the film cooling zone) those computed in the uncooled expansion.

The gas outlet total enthalpy ($h_{t,g,am}$) is calculated through an energy balance, considering the mixing between the expanding fluid and the cooling mass flow rate and the thermal power transferred across the blade wall ($\dot{m}_c \cdot \Delta h_{t,c}$). This term appears only in the film cooling zone balance and it is estimated by using the values of ξ and η computed during the previous iteration.

$$\dot{m}_g h_{t,g,i} + r_{fc}\dot{m}_c h_{t,c,o} = \\ = \left(\dot{m}_g + r_{fc}\dot{m}_c\right) h_{t,g,am} + \dot{m}_c \Delta h_{t,c} \tag{5}$$

Then, the gas outlet velocity ($v_{g,am}$) is updated using the momentum balance (Eq. (6)) and assuming that: the mixing process takes place at the blade exit (i.e., after the heat transfer process), the cooling injection does not change the direction of the gas outlet velocity (calculated for the uncooled version) and the cross-flow component of the coolant injection kinetic energy is lost.

$$\left(\frac{p_{g,o}}{\rho_{g,o} v_{g,o}} + v_{g,o}\right)\dot{m}_g + r_{fc}\dot{m}_c v_{c,o}\cos(\alpha) = \\ = \left(\frac{p_{g,am}}{\rho_{g,am} v_{g,am}} + v_{g,am}\right) \cdot \\ \cdot \left(\dot{m}_g + r_{fc}\dot{m}_c\right) \tag{6}$$

At this point, the average gas properties during the heat transfer process can be computed and the average heat transfer coefficient at the gas side is computed decomposing the blade in three sections, as described by Simon and Piggush [19]. The leading edge is modeled as a cylinder in cross flow (Eq. (7)) and the pressure and suction sides as flat surfaces (Eq. (8)).

$$\frac{h_\theta D_0}{k_g} = 1.14\left(\frac{\rho_g v_\infty D_0}{\mu_g}\right)^{0.5} Pr_g^{0.4} \cdot \\ \cdot \left[1 - \left(\frac{\theta}{90}\right)^3\right] \tag{7}$$

$$\frac{h_x}{\rho_g c_{p,g} v_\infty} = 0.0296 Re_x^{-0.2} Pr_g^{-2/3} \tag{8}$$

Eqs. (7) and (8) are integrated along the blade and then the weighted average, based on the fractions of total surface area of a simple blade profile and assuming that the actual geometry has a small effect on the weight coefficients, is determined.

The film cooling reference temperature is calculated as suggested by Goldstein et al. [20] and the film cooling efficiency is evaluated by means of the semi-empirical correlation proposed by Goldstein and Haji-Sheikh [21] (Eq. (9)). Then, its definition (Eq. (10)) is used to compute the adiabatic wall temperature (T_{aw}), which is required to calculate the thermal power exchanged between the hot gas and the blade wall.

$$\eta_{fc} = \left\{1.9 Pr_{gf}^{2/3}\right\} / \left\{1 + 0.329\frac{c_{p,gf}}{c_{p,c}} \cdot \right. \\ \cdot Re_{gf}^{-0.2}\left(\frac{x}{c}\right)^{0.8}\left[\frac{2a_t\sigma}{\Psi_g}\frac{\dot{m}_g}{r_{fc}\dot{m}_c} + \right. \\ \left.\left. + 0.00015 Re_{gf}\frac{W_g}{W_c}\sin(\alpha)\right]\right\} \tag{9}$$

$$\eta_{fc} = \frac{T_{g,i} - T_{aw}}{T_{g,i} - T_{c,o}} \tag{10}$$

Finally, an updated value of the ratio between the coolant (assumed at the first iteration) and mainstream mass flow rate (ξ) can be computed using the energy balance of the heat transfer process (Eq. (11)).

$$\xi = \lambda\left(\frac{1}{h_g} + \frac{t_{TBC}}{k_{TBC}}\right)^{-1}\frac{1}{\rho_g v_{g,am}} \cdot \\ \cdot \frac{T_{aw} - T_{bmax}}{\Delta h_{t,c}} \tag{11}$$

The iterative process continues from Eq. (1) to (11) by updating the values of the guessed parameters (ξ and η) using a direct substitution method. Convergence is reached in 10 - 50 iterations, depending on the blade row geometry and input data.

For the rotor blade row, the same procedure is used with the only differences of replacing the enthalpy in the energy balances with the rothalpy, and evaluating the total properties using the relative velocities.

Note that the model does not estimate the cooling flow requirement of the casing and disks, which however can be as high as one percentage point of the inlet mainstream mass flow rate for each cooled stage [22].

Table 1: Working fluid composition.

Compound	Molar fraction
CO_2	0.9314
H_2O	0.0500
N_2	0.0112
Ar	0.0054
O_2	0.0020
Total	1.0000

4. CASE STUDY

The case studied in this article has been derived from the optimized case presented in Scaccabarozzi et al. with the constraint of a maximum turbine outlet temperature of 998.15 K. The resulting turbine operating conditions are:

- Inlet mass flow rate: 1214.38 kg/s.
- Total inlet pressure: 30.695 MPa.
- Total inlet temperature: 1427.27 K.
- Total outlet pressure: 3.06 MPa.
- Coolant inlet temperature: 429.63 K.

The working fluid composition is reported in Table 1.

To achieve the specified turbine outlet total pressure it is assumed that a hypothetical diffuser would allow recovering 90 % of the axial kinetic energy difference regained by an ideal process [23] (assuming A_o/A_i ratio of 2.5), while the tangential velocity component is completely wasted.

The computation has been carried out first for the uncooled case and then for the cooled turbine in order to compare the results and assess the impact of the cooling system on both the performance and outlet conditions. Both cases have been designed under the same assumption, using the same reaction degree (0.5), flow coefficient (0.6) and work coefficient (2.5) for each stage, as recommended by the Smith's chart, to obtain a good stage efficiency while reasonably distributing the work extraction among the stages. Furthermore, a 20 % linear increase of the mean diameter throughout the whole machine and a minimum ratio between the blade height and the mean diameter equal to 0.05 have been assumed. These allow the less critical stages from a thermo-mechanical point of view (the last ones) to increase the power extraction, proportional to the peripheral velocity and thus to the mean diameter, while avoiding excessive annular losses, related to the ratio between the blade height and the mean diameter, on the most critical ones (the first one).

For the cooled case, the analysis has been performed assuming that the stages can use both the film cooling and a protective thermal barrier coating (0.2 mm thickness, similarly to gas turbine ones) to minimize the amount of cooling flow requirement and maintain a maximum allowed temperature of the blade metal of 1133.15 K as specified in [5].

Regarding the turbine performance, comparing the total-static and total-total efficiency of the cooled and uncooled turbines may be misleading because the injection of the cold cooling flows causes a reduction of the outlet entropy and enthalpy. For this reason, the comparison between the cooled and uncooled turbine performance should be made considering as reference for the calculation of the total-static efficiency the adiabatic availability of the system [24]. For the uncooled turbine, the adiabatic availability corresponds to the conventional total-static isentropic enthalpy drop while for the cooled turbine it represents the work produced by a reversible adiabatic device which expands to the outlet pressure and mixes (in a reversible process) the two inlet streams (the hot gas and the cooling flows). The

Table 2: Cooling system performance results.

Blade row	ξ %	η %	η_{fc} %	ΔT_{TBC} K	$T_{c,o}$ K
Stator 01	0.85	9.18	11.99	140.44	494.23
Rotor 01	0.72	10.82	10.70	125.83	505.73
Stator 02	0.57	14.32	9.12	111.30	530.40
Rotor 02	0.42	16.52	7.89	95.93	545.84
Stator 03	0.34	23.81	6.27	84.51	597.11
Rotor 03	0.22	31.33	5.00	69.55	650.01
Stator 04	0.18	43.46	3.69	54.84	735.36
Rotor 04	0.10	57.87	2.52	38.77	836.76
Stator 05	0.06	70.18	1.30	21.07	923.38
Rotor 05	0.01	91.70	0.26	4.27	1 074.72
Stator 06	-	-	-	-	-
Rotor 06	-	-	-	-	-

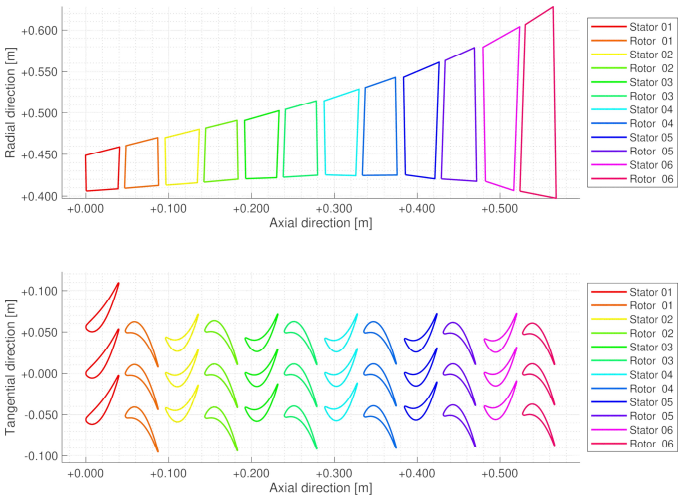

Figure 2: a) (top) Cooled turbine cross sectional view. b) (bottom) Cooled turbine mid-span blade profile view

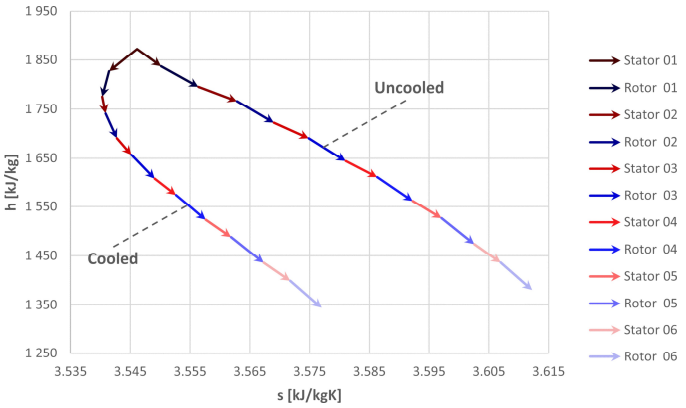

Figure 3: Specific enthalpy - specific entropy expansion diagram for the uncooled (right) and cooled (left) cases.

total static efficiency referred to the adiabatic availability can be evaluated using Eq. (12). To determine the isentropic outlet enthalpy, it is necessary to consider that the outlet entropy of the mixed stream (inlet stream + cooling flows) is equal to the weighted average entropy of the inlet contributions (this results from the entropy balance equation for a reversible process).

$$\eta_{ad,ts} = \frac{\Delta h_{tt}^{real}}{h_{t,g,i} - h\left(p_{g,o}, \frac{\dot{m}_g s_{g,i} + \dot{m}_c s_{c,i}}{\dot{m}_g + \dot{m}_c}\right)} \quad (12)$$

5. RESULTS

The results related to the cooling system performance are shown in Table 2. Note that all the blade rows require a cooling flow (ξ) smaller than 1 % of the inlet gas mass flow rate. The coolant mass flow rate decreases during the expansion, while the heat transfer area increases (due to the increase in blade height and size) causing a progressively higher coolant temperature at the blade exit ($T_{c,o}$). This directly affects the overall cooling efficiency (η), which increases from 9.18 % to 91.70 %.

Another remarkable result concerns the film cooling effectiveness values (always lower than 12 %), which are significantly lower than the ones reported in the literature for a conventional gas turbine, where it can be as high as 40 % [9]. This difference can be attributed to the significantly higher density of the working fluid expanding in the Allam cycle turbine which leads to higher Reynolds number of the mainstream. As reported in Eq. (9), having high Reynolds numbers decreases the film cooling effectiveness (note that the other terms of the equation are not significantly different from a conventional gas turbine).

As for conventional machines operating with high temperature working fluid, from Table 2 it can be seen that the thermal barrier coating is significantly useful for the high temperature stages allowing an external surface temperature more than one hundred Kelvin higher than the maximum metal value.

Figure 2 shows the cross-sectional view and the blade-to-blade view of the cooled turbine. The blade profile geometry was derived using the blade modeler Stagen developed by the Whittle Lab [25]. Note that the

Table 3: Total-static and total-total adiabatic efficiency of each stage and of the overall expansion for both the uncooled and the cooled cases.

	Uncooled case		Cooled case	
	$\eta_{ad,ts}$ %	$\eta_{ad,tt}$ %	$\eta_{ad,ts}$ %	$\eta_{ad,tt}$ %
Stage 01	70.28%	82.88%	61.72%	71.64%
Stage 02	69.36%	81.44%	64.38%	75.01%
Stage 03	71.01%	83.71%	68.24%	80.15%
Stage 04	72.68%	86.02%	71.52%	84.56%
Stage 05	74.29%	88.27%	74.07%	88.03%
Stage 06	75.61%	90.11%	75.68%	90.19%
Overall	84.57%	87.60%	81.79%	84.64%

presented blade profile does not influence the results presented in this work.

Due the selected design criteria of adopting the same reaction degree, flow coefficient and work coefficient for all the stages, all the stages (excluding the first stage stator) of the cooled and uncooled turbines have the same blade profiles and very similar velocity triangles.

Figure 3 shows the expansion transformations of the main stream in the specific enthalpy - specific entropy diagram. The transformation on the left refers to the cooled turbine while the one on the right refers to the uncooled turbine. It is worth noting the decrease of entropy of the main stream across the first stator and rotor caused by the heat transferred to the cooling flows.

Comparing the performances referred to the adiabatic availability of the process, reported in Table 3, it is possible to quantify the negative thermo-fluid-dynamic effect of the cooling system on the overall expansion. The penalty due to cooling starts as high as around 8.5 percentage points for the first stage (i.e. total-static efficiency of 70.3 % for the uncooled vs 61.7 % for the cooled machine) and progressively decreases due to the gradually reducing coolant mass flow rate and its higher blade outlet temperature. For the last stage, since it is not cooled, the adiabatic efficiency is essentially the same for the cooled and uncooled turbines. Overall, the cooled turbine loses about 2.8 percentage points of efficiency (either total-static or total-total) compared to the uncooled turbine.

6. CONCLUSIONS

A methodology for the preliminary thermo-fluid-dynamic design and performance estimation of the supercritical Allam cycle CO_2-based turbine is presented. The model is based on the integration between a 1D mean-line code for row-by-row geometrical fluid-dynamic design with an extended model for the assessment of the cooling requirements. Once the cooling mode has been selected among convective, film cooling or thermal barrier coating (or a combination of them), the model provides a preliminary estimate of the coolant mass flow rates, as well as a quantification of performance losses within each row. Simulations for a relevant case (i.e., 6-stage, full scale, around 600 MW_{el}, Allam cycle turbine) and comparison between cooled vs. uncooled expander highlights that:

- 5 stages out of 6 needs to be cooled to preserve the blades integrity (i.e., T_{bmax}).
- Compared to a large-scale, air-breathing natural gas-fired gas turbine with the same power output, the CO_2 expander features smaller tip diameter (i.e., 1.2 m maximum), mainly due to the denser working fluid.
- Film cooling is much less effective compared to conventional gas turbines because of the higher density of the working fluid.
- Cooling significantly affects the expansion efficiency, which is penalized by 2.8 percentage points.
- The turbine efficiency and cooling flow requirements for the blades (excluding discs) computed in this work well matches the value reported in [5], supporting the conclusion that the Allam cycle could efficiently produce power with near-zero emissions.

REFERENCE

[1] Rao AD. Combined Cycle Systems for Near-Zero Emission Power Generation. Woodhead Publishing; 2012.

[2] Ferrari N, Mancuso L, Davison J, Chiesa P, Martelli E, Romano MC. Oxy-turbine for Power Plant with CO2 Capture. Energy Procedia 2017;114:471–80. doi:10.1016/j.egypro.2017.03.1189.

[3] Allam RJ, Palmer MR, Brown GW, Fetvedt JE, Freed DA, Nomoto H, et al. High Efficiency and Low Cost of Electricity Generation from Fossil Fuels While Eliminating Atmospheric Emissions, Including Carbon Dioxide. Energy Procedia 2013;37:1135–49. doi:10.1016/j.egypro.2013.05.211.

[4] Scaccabarozzi R, Gatti M, Martelli E. Thermodynamic Optimization and Part-load Analysis of the NET Power Cycle. Energy Procedia 2017;114:551–60. doi:10.1016/j.egypro.2017.03.1197.

[5] Scaccabarozzi R, Gatti M, Martelli E. Thermodynamic analysis and numerical optimization of the NET Power oxy-combustion cycle. Appl Energy 2016;178:505–26. doi:10.1016/j.apenergy.2016.06.060.

[6] Allam R, Martin S, Forrest B, Fetvedt J, Lu X, Freed D, et al. Demonstration of the Allam Cycle: An Update on the Development Status of a High Efficiency Supercritical Carbon Dioxide Power Process Employing Full Carbon Capture. Energy Procedia 2017;114:5948–66. doi:10.1016/j.egypro.2017.03.1731.

[7] Sasaki T, Itoh M, Maeda H, Tominaga J, Saito D, Niizeki Y. Development of Turbine and Combustor for a Semi-Closed Recuperated Brayton Cycle of Supercritical Carbon Dioxide. Vol. 1 Boil. Heat Recover. Steam Gener. Combust. Turbines; Energy Water Sustain. Fuels, Combust. Mater. Handl. Heat Exch. Condens. Cool. Syst. Balanc., ASME; 2017, p. V001T02A008. doi:10.1115/POWER-ICOPE2017-3419.

[8] Denton JD. The 1993 IGTI Scholar Lecture: Loss Mechanisms in Turbomachines. J Turbomach 1993;115:621. doi:10.1115/1.2929299.

[9] Horlock JH, Watson DT, Jones T V. Limitations on Gas Turbine Performance Imposed by Large Turbine Cooling Flows. J Eng Gas Turbines Power 2001;123:487–94. doi:10.1115/1.1373398.
[10] Torbidoni L, Massardo AF. Analytical Blade Row Cooling Model for Innovative Gas Turbine Cycle Evaluations Supported by Semi-Empirical Air-Cooled Blade Data. J Eng Gas Turbines Power 2004;126:498. doi:10.1115/1.1707030.
[11] El-Masri MA. On Thermodynamics of Gas-Turbine Cycles: Part 2—A Model for Expansion in Cooled Turbines. J Eng Gas Turbines Power 1986;108:151–9. doi:10.1115/1.3239862.
[12] Pini M, Persico G, Casati E, Dossena V. Preliminary Design of a Centrifugal Turbine for Organic Rankine Cycle Applications. J Eng Gas Turbines Power 2013;135:042312. doi:10.1115/1.4023122.
[13] Bahamonde S, Pini M, De Servi C, Rubino A, Colonna P. Method for the Preliminary Fluid Dynamic Design of High-Temperature Mini-Organic Rankine Cycle Turbines. J Eng Gas Turbines Power 2017;139:082606. doi:10.1115/1.4035841.
[14] Colonna P, van der Stelt T, Guardone AMA. FluidProp (Version 3.0): A program for the estimation of thermophysical properties of fluids 2012.
[15] Kunz O, Wagner W. The GERG-2008 Wide-Range Equation of State for Natural Gases and Other Mixtures: An Expansion of GERG-2004. J Chem Eng Data 2012;57:3032–91. doi:10.1021/je300655b.
[16] Traupel W. Thermische Turbomaschinen. Berlin, Heidelberg: Springer Berlin Heidelberg; 1982. doi:10.1007/978-3-642-96632-3.
[17] Zweifel O. The spacing of turbo-machine blading especially with large angular deection. Brown Boveri Rev 1945;32:436–444.
[18] Dittus FW, Boelter LMK. Heat transfer in automobile radiators of the tubular type. Int Commun Heat Mass Transf 1985;12:3–22. doi:10.1016/0735-1933(85)90003-X.
[19] Simon T, Piggush J. Hot gas path heat transfer characteristics / active cooling of turbine components. In: Amano RS, Sundén B, editors. Therm. Eng. Power Syst., Ashurst, Southampton, UK: WIT Press; 2008, p. 231–303.
[20] Goldstein RJ, Eckert ERG, Wilson DJ. Film Cooling With Normal Injection Into a Supersonic Flow. J Eng Ind 1968;90:584. doi:10.1115/1.3604692.
[21] Goldstein RJ, Haji-Sheikh A. Prediction of Film Cooling Effectiveness. Proc. 1967, Semi-International Symp. (Tokyo), Japan Soc. Mech. Eng., Tokyo: 1967, p. 213–218.
[22] Chiesa P, Macchi E. A Thermodynamic Analysis of Different Options to Break 60% Electric Efficiency in Combined Cycle Power Plants. J Eng Gas Turbines Power 2004;126:770–85. doi:10.1115/1.1771684.
[23] Dixon SL, Hall C. Fluid Mechanics and Thermodynamics of Turbomachinery. 7th ed. Butterworth-Heinemann; 2014.
[24] Gyftopoulos EP, Beretta GP. Thermodynamics: Foundations And Applications. New York City, New York, U.S.: 2005.
[25] Denton JD. Multall—An Open Source, Computational Fluid Dynamics Based, Turbomachinery Design System. J Turbomach 2017;139:121001. doi:10.1115/1.4037819.